

Strong-Coupling Modification of Singlet-Fission Dynamical Pathways

Lisamaria Wallner,^{*,†} Charlotte Remnant,[†] and Oriol Vendrell^{*,†,‡}

[†]*Theoretische Chemie, Physikalisch-Chemisches Institut, Universität Heidelberg, Im
Neuenheimer Feld 229, 69120 Heidelberg, Germany*

[‡]*Interdisciplinary Center for Scientific Computing, Universität Heidelberg, Im
Neuenheimer Feld 205, 69120 Heidelberg, Germany*

E-mail: l.wallner@stud.uni-heidelberg.de; oriol.vendrell@uni-heidelberg.de

Abstract

We investigate theoretically the influence of strong light-matter coupling on the initial steps of the photo-triggered singlet-fission process. In particular we focus on intra-molecular singlet fission in a TIPS-pentacene dimer derivative described by a vibronic Hamiltonian including the optically active singlet excited states, doubly excited and charge transfer states, as well as the final triplet-triplet pair state. Quantum dynamics simulations of up to four dimers in the cavity indicate that the modified resonance condition imposed by the cavity strongly quenches the passage through the intermediate charge transfer and double-excitation states, thus largely reducing the triplet-triplet yield in the bare system. Subsequently, we modify the system parameters and construct a model Hamiltonian where the optically-active singlet excitation lies below the final triplet-triplet state such that the yield of the bare system becomes insignificant. In this case we find that using the upper polariton as the doorway state for photo-excitation can lead to a much enhanced yield. This pathway is operative provided that the system is sufficiently rigid to prevent vibronic losses from the upper polariton to the dark-states manifold.

Introduction

Recent efforts in the understanding of strong light-matter interaction in optical cavities have brought to light diverse field-induced modifications of chemical properties, including modified thermal chemistry, photochemistry, as well as transport phenomena in materials.¹⁻⁶ These modifications are attributed to the formation of light-matter hybrid states, so called polaritons. Exciton-polaritons, thus formed by the combination of electronic excitations with light, have been shown to alter the properties of the bare excitonic systems, influencing processes like electron transport,⁷⁻⁹ light-harvesting^{10,11} or energy transfer.^{2,4} Among these, singlet fission (SF) is an important photophysical process for light-harvesting applications that can be used to circumvent the Shockley-Queisser efficiency limit thereby increasing

the external quantum efficiency of organic solar cells.¹²⁻¹⁴ In SF a singlet exciton (SE) converts into a multiexcitonic (ME) state consisting of a correlated triplet pair state with singlet character, thus being a spin-allowed process where least two molecules, or molecular fragments in the case of internal singlet fission (iSF), must be involved. The triplet pair state eventually decoheres and separates to form two independent triplet excitons localized on two different molecules or molecular fragments.¹⁵⁻¹⁷ A wide exploitation of SF for solar energy conversion remains challenging, though, as only a limited number of materials can display this phenomenon.¹⁸⁻²⁰ In particular, monomers with good characteristics for SF must feature a triplet state at an energy slightly below half of the first singlet excitation, such that one singlet excited state can transfer into two separate triplets resonantly. Unfortunately, it is challenging to control this energetic boundary condition intrinsically, since it depends to a large extent on the electronic structure of the corresponding monomers.

Therefore, the utilization of exciton-polaritons represents an appealing strategy to modify the SF characteristics of materials. A number of experimental studies have already been conducted on how strong light-matter coupling affects the SF process in different types of cavities.^{11,21-25} For instance, amorphous rubrene thin films under strong-coupling showcased a field-induced decoupling effect, thereby suppressing SF.²² Additionally, polariton-mediated enhancement of light harvesting in TIPS-tetracene thin films was observed.¹¹ Furthermore, studies have been conducted that examine the interaction between polaritonic effects and SF near metallic surfaces. The findings indicate that the dynamics remained unchanged in the presence of polaritons.^{25,26}

Theoretical studies have investigated the impact of strong coupling on SF systems, with a particular focus on the direct SF pathways within fundamental three-state models, which comprise the ground state (GS), singlet excited state (SE), and the final multiexcitonic (ME) state.²⁷⁻²⁹ Higher-lying electronic states, particularly the charge transfer (CT) states, have been included in some of the polaritonic models in recognition of their significance in the SF process.^{30,31} These states, in addition to the high-lying doubly excited states, play a crucial

role in the SF process through indirect pathways.³²

In order to engineer the optimal passage through these dynamical pathways, the effect of the cavity on the transient population of the intermediate states needs to be well understood. In addition, the coupling to the cavity results in new bright resonances centered around the lower and the upper polaritonic states, which can be used as doorway states to initiate the SF process. The specificities of starting through either resonance can be investigated by considering explicit laser pulses tuned to specific resonances of the absorption spectrum.³³

Hence, here we consider a realistic model for iSF that incorporates both the high-lying charge transfer (CT) and doubly excited (DE) states, with the objective of comprehensively capturing their influence on the modified SF mechanism through full quantum dynamics simulations and the consideration of collective effects. Through the inclusion of the femtosecond excitation laser-pulse tuned to specific resonances in the model we can carefully investigate the how the different doorway states result in different dynamics and finally different yields. Additionally, we examine in some detail the possibility of using the upper polariton as a doorway. This strategy may be beneficial for materials where the first singlet excited state is energetically too low compared to twice the triplet excitation energy, which is the case for smaller organic systems. A significant number of molecular systems exhibit this energy distribution,¹⁹ and in general smaller molecules may be more robust towards degradation processes and easier to prepare and produce.

Theory and Methods

Polaritonic-Molecular Hamiltonian

We consider N molecules strongly coupled to a cavity mode and described by the Hamiltonian

$$\hat{H} = \sum_{n=1}^N \hat{H}_{\text{mol}}^{(n)} + \hat{H}_{\text{cav}} + \hat{H}_{\text{las}}, \quad (1)$$

where $\hat{H}_{\text{mol}}^{(n)}$ is the n -th molecular Hamiltonian, \hat{H}_{cav} is the cavity Hamiltonian and \hat{H}_{las} describes a laser pulse interacting with the system. The molecular Hamiltonian is considered in its general diabatic representation

$$\hat{H}_{\text{mol}}^{(n)} = \hat{T}^{(n)} + \sum_{i,j=1}^{N_e} |i_n\rangle W_{ij}(\mathbf{Q}^{(n)}) \langle j_n|, \quad (2)$$

where N_e is the number of intramolecular electronic states considered for each molecule,

$$W_{ij}(\mathbf{Q}^{(n)}) = \langle \varphi_i^{(n)} | \hat{H}_{\text{el}}(\mathbf{r}^{(n)}, \mathbf{Q}^{(n)}) | \varphi_j^{(n)} \rangle \quad (3)$$

are the matrix elements of the electronic Hamiltonian in the basis of local diabatic states for the n -th molecule, and the brackets indicate integration over the local electronic coordinates $\mathbf{r}^{(n)}$. The coupling to the quantized electromagnetic mode of the cavity is considered in Coulomb gauge and length form^{34,35}

$$\hat{H}_{\text{cav}} = \hbar\omega_c (\hat{a}^\dagger \hat{a}) + \sqrt{\frac{\hbar\omega_c}{2}} \lambda \vec{\varepsilon}_c \vec{D} (\hat{a}^\dagger + \hat{a}) + \frac{1}{2} (\lambda \vec{\varepsilon}_c \vec{D})^2, \quad (4)$$

where ω_c is the cavity frequency. The second term describes the linear interaction between the molecule and the cavity, where $\vec{\varepsilon}_c$ is the polarization vector of the cavity mode and $\lambda = \sqrt{1/\varepsilon_0 V}$ is the coupling strength with quantization volume V and vacuum polarization ε_0 . As usual, to facilitate comparisons we introduce the coupling parameter $g = \lambda\sqrt{\hbar\omega_c}/2$ with units of electric field. $\vec{D} = \sum_{n=1}^N \vec{\mu}$ is the total dipole operator of the molecular ensemble.

In case we need to describe the interaction with an external laser pulse k explicitly, we introduce it for convenience through its vector potential, $\vec{E}_k(t) = -\partial \vec{A}_k(t)/\partial t$,

$$A_k(t) = \vec{\varepsilon}_k \frac{E_{k,0}}{\omega_k} \exp \left[-\frac{2\ln 2}{F^2} (t - \tau_k)^2 \right] \cos(\omega_k(t - \tau_k)), \quad (5)$$

where $E_{k,0}$ is the field amplitude, ω_k and $\vec{\varepsilon}_k$ are the carrier frequency and polarization direc-

tion of the laser pulse, F corresponds to the FWHM of the intensity profile, and τ_k is the center of the pulse. The corresponding interaction Hamiltonian in the dipole approximation then reads $\hat{H}_{\text{las}} = -\vec{D} \cdot \vec{E}_k(t)$.

Hamiltonian 4 corresponds to the Pauli-Fierz description of light-matter interaction in the case that the molecules interact with a single effective electromagnetic mode. From the perspective of the material system, the main approximation in our treatment corresponds to the introduction of a local basis of field-free molecular states for each monomer, on which all relevant operators are represented. For a given set of electromagnetic modes and coupling parameter λ , the scheme outlined above is formally exact as long as the local molecular basis can be considered to be complete.

Intramolecular Singlet Fission Model in a Cavity

The simulations on iSF reported here are based on the vibronic Hamiltonian of *o*-bis(13-(methylethynyl)pentacen-6-yl)ethynyl)benzene dimer (*o*-TIPSPm) parametrized by Reddy and Thoss,³² which they simulated using the multilayer multiconfiguration time-dependent Hartree method (ML-MCTDH).³⁶⁻³⁸ This model considers the 8 most important electronic states in the iSF process of the *o*-TIPSPm, namely the electronic ground state (GS), the first two locally excited states (LE), two high-lying charge transfer states (CT) and two doubly excited states (DE), as well as the final multiexcitonic (TT) state. The diabatic electronic Hamiltonian for this window of electronic states at the Franck-Condon geometry $\mathbf{Q}^{(n)} = 0$ is reproduced from Ref. 32 in Table 1. Their model also considers the 8 fundamental vibrational modes for the iSF process and their respective linear and quadratic vibronic couplings, selected by Reddy and Thoss,³² to account for the non-adiabatic effects. The vibrations consist of mostly ring-breathing and -stretching modes that involve the pentacene subunits. The LE states of this model are then coupled to a resonant cavity photon according to Eq. 4.

Table 1: Diabatic electronic Hamiltonian matrix of *o*-TIPSPm at the FC point, $Q^{(n)} = 0$. Energies in [meV] reproduced from Ref. 32

	${}^1(S_0S_0)$	${}^1(T_1T_1)$	${}^1(S_0S_1)$	${}^1(S_1S_0)$	${}^1(CA)$	${}^1(AC)$	${}^1(DE)_1$	${}^1(DE)_2$
${}^1(S_0S_0)$	-174.3	23.0	-28.5	36.6	19.2	-16.2	377.9	380.3
${}^1(T_1T_1)$	23.0	1951.8	4.4	-8.8	-202.5	200.5	-16.3	-13.3
${}^1(S_1S_0)$	-28.5	4.4	1564.4	-36.3	13.9	24.2	39.9	9.0
${}^1(S_0S_1)$	36.6	-8.8	-36.3	1555.7	26.4	14.0	-12.6	-43.8
${}^1(CA)$	19.2	-202.5	13.9	26.4	1827.7	27.2	54.9	37.3
${}^1(AC)$	-16.2	200.5	24.2	14.0	27.2	1829.6	-38.3	-53.4
${}^1(DE)_1$	377.9	-16.3	39.9	-12.6	54.9	-38.3	2135.2	-126.2
${}^1(DE)_2$	380.3	-13.3	9.0	-43.8	37.3	-53.4	-126.2	2113.5

MCTDH Dynamics and Analysis

The time-dependent Schrödinger equation for the molecules-cavity system was integrated using the MCTDH approach^{39,40} in its multilayer generalization^{36–38} using the MCTDH Heidelberg package.⁴¹ The treatment of molecular ensembles coupled to cavity modes using the ML-MCTDH approach has been described in some detail in Ref. 42 and used in several applications.^{33,42} In particular, it is most convenient when considering an ensemble of molecules that each molecule has its own separate electronic and vibrational degrees of freedom. This allows for layering schemes of the ML tree where each molecule "lives" in a separate sub-tree, the advantage being that the strongest correlations are within the molecules themselves compared to the cavity-molecules coupling. Examples of the tensor trees used in the simulations are found in the Appendix. The primitive degrees of freedom of each molecule are treated using the same grids as in Ref. 32.

In order to follow the dynamics of the coupled electronic and cavity states we define the upper and lower polaritons using their amplitudes at exact resonance

$$|\psi_{\pm}\rangle = \frac{1}{\sqrt{2}}|1, 0\rangle \pm \frac{1}{\sqrt{2N}} \sum_{k=1}^N |0, k_{+}\rangle. \quad (6)$$

Here $|1, 0\rangle$ indicates an excitation in the cavity while no molecules are excited and $|0, k_{+}\rangle$ corresponds to the unexcited cavity and a bright exciton in the k -th molecule. Specifically,

since each molecule corresponds to an excitonic dimer, one can introduce the bright and dark local excitations

$$|0, k_{\pm}\rangle = \frac{1}{\sqrt{2}} (|0, k_{10}\rangle \pm |0, k_{01}\rangle) \quad (7)$$

where $|0, k_{10}\rangle$ corresponds to the k -th dimer with the first monomer excited, and so on. Following these definitions one can introduce projectors onto the specific subspaces, for example $\hat{P}_{\pm} = |\psi_{\pm}\rangle\langle\psi_{\pm}|$.

When simulating the dynamics triggered by an explicit laser pulse we define triplet-triplet yield of dimer k as

$$Y_k = \frac{P_{\text{ME}}^{(k)}(t)}{1 - P_{00}^k(t)}, \quad (8)$$

where $P_{\text{ME}}^{(k)}(t)$ indicates the population of the final ME state of dimer k at time t and $P_{00}^k(t)$ is the corresponding population of the electronic ground state. Since all dimers are identical, and the dynamics takes place within the single-excitation manifold, it follows that $Y = N \cdot Y_k$.

Alternatively, one can start the dynamics either initially populating the cavity, populating the molecules coherently, or populating either the upper or lower polaritons. For the latter, one applies the transition operator³³

$$\hat{T}_{\pm} = \frac{1}{\sqrt{2}} \left(\hat{a}^{\dagger} \pm \frac{1}{\sqrt{N}} \sum_{k=1}^N \left(\frac{\hat{\sigma}_{k,01}^{\dagger} + \hat{\sigma}_{k,10}^{\dagger}}{\sqrt{2}} \right) \right) \quad (9)$$

where the ladder operators above are defined by

$$\hat{a}^{\dagger}|0, 0\rangle = |1, 0\rangle \quad (10)$$

$$\hat{\sigma}_{k,01}^{\dagger}|0, 0\rangle = |0, k_{01}\rangle \quad (11)$$

$$\hat{\sigma}_{k,01}^{\dagger}|0, 0\rangle = |0, k_{01}\rangle. \quad (12)$$

Absorption spectra were calculated by Fourier transform of the autocorrelation function of the dipole-operated ground state or the ground state operated with some specific transition operator as defined above.

Results and Discussion

Modified Intramolecular Singlet Fission in the *o*-TIPSm dimer

First we consider a single dimer coupled to the cavity and four coupling strengths $\tilde{g}/\omega_c = (5 \cdot 10^{-3}, 1 \cdot 10^{-2}, 4 \cdot 10^{-2}, 6 \cdot 10^{-2})$. We note that the \tilde{g} is assumed to be already multiplied with the molecular transition dipole matrix element, and in the following we refer to this parameter as g . For each coupling strength, the corresponding electronic absorption spectrum calculated from the autocorrelation function of the dipole-operated ground states is shown in Fig. 1a. It can be seen how the Rabi splitting increases with the coupling strength, resulting in clearly separated UP and LP resonances for $g/\omega_c = 4 \cdot 10^{-2}$ and larger couplings. These absorption lines, indicated by the small vertical lines in Fig. 1a, were targeted by a laser pulse with carrier frequency resonant with the center of the corresponding absorption band and spectral bandwidth (fwhm) of 0.02 eV and the duration of the laser pulse is set to 90 fs. The amplitude of the laser was set to ensure that the excitation remained within the one-photon regime.³³

The different propagations initiated by the explicit laser pulses targeted the UP and LP bands at all coupling strengths. The cavity was set in all cases resonant with the first singlet excitation of the dimer at $\omega_c = 1.75$ eV and the laser frequencies are given in the caption of Fig. 1. Irrespective of the coupling strength of the cavity and the laser frequency ω_L , coupling to the cavity decreased the population transfer to the final triplet-triplet ME state in all instances compared to the bare system, as seen in Fig. 1b.

The effect of the cavity on the electronic structure of the dimer turns out to be not so simple. Inspecting the cut of the adiabatic PESs along the tuning vibrational mode Q_{19} ,

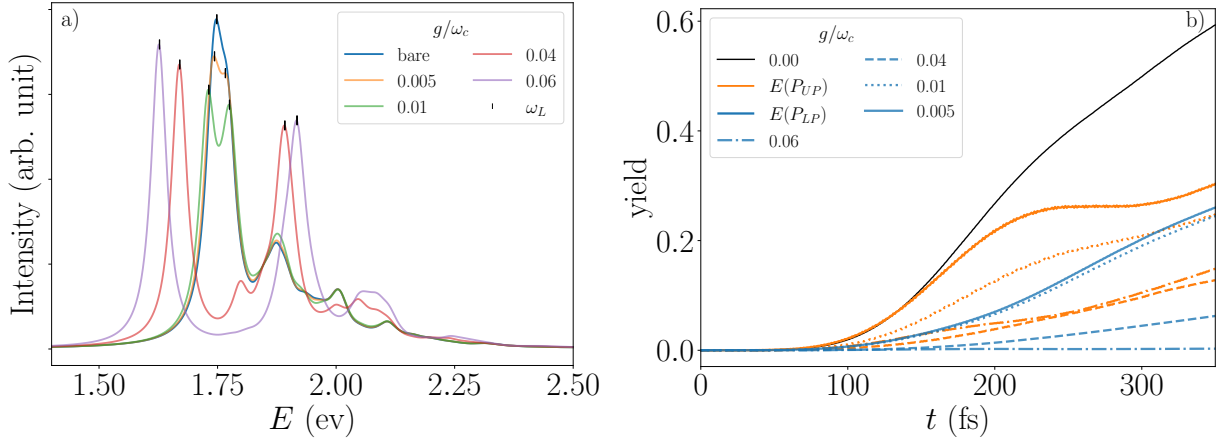


Figure 1: (a) Absorption spectra of the bare *o*-TIPSm dimer and the dimer coupled to the cavity at various coupling strengths. The small vertical lines indicate the photon energy $\omega_L = (1.626 \text{ eV}, 1.669 \text{ eV}, 1.730 \text{ eV}, 1.743 \text{ eV}, 1.747 \text{ eV}, 1.765 \text{ eV}, 1.774 \text{ eV}, 1.891 \text{ eV}, 1.915 \text{ eV})$ from left to right, of the corresponding simulations targeting the bright absorption lines. (b) Comparison of the singlet fission yield of the bare molecule and the cavity-coupled molecule for different coupling strengths after laser excitation. The blue lines represent the yield after excitation to the UP state, while the orange lines represent the yield after excitation to the LP state. The fast Rabi oscillations were smoothed by taking a running average over 10 femtoseconds.

Fig. 2, we can identify two parallel polaritonic PES with substantial photonic character, the LP and UP, which cross the curve leading to the minimum energy geometry of the ME state, but also present avoided crossings with the intermediate adiabatic states. In order to better understand the dynamics leading to the reduced yield, we start simulations selectively from the UP and LP states using the transition operators in Eq. 9, and compare them to the time evolution of the bare system started from the bright excitonic state of the dimer. In the analysis, the electronic-photonic population is split into three subspaces. The first subspace contains only the final diabatic ME state. The second subspace contains all diabatic states directly involved with the light-matter interaction, namely the ground and singlet excited electronic states of the dimer plus the one-photon excitation of the cavity (in the bare system the latter state is obviously absent). The third subgroup encompasses the four intermediate DE and CT electronic states.

In the bare system, photo-excitation of the singlet resonance results in quick population

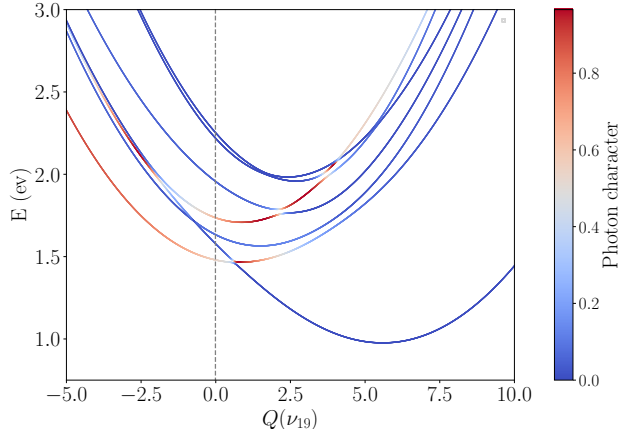


Figure 2: Cut of the adiabatic polaritonic surface along mode Q_{19} with a coupling strength of 0.06 where the gradient indicates the character of the state. The gray dashed line shows the position of the Franck-Condon point. For the sake of clarity, the ground state is not shown in this plot.

transfer to the intermediate states (green trace in Fig. 3a) which subsequently drifts towards the final ME state. Exciting the UP results in a reduced population transfer to the intermediate states, and between 50 to 70% of the population stays trapped in the polaritonic subsystem (orange trace in Fig. 3b), and would ultimately decay as photon losses.⁴³ Excitation of the LP state results in a complete suppression of the population transfer to the intermediate states, which are then too high in energy with respect to the lower polaritonic excitation. This example illustrates the energy shift effect of the polaritonic excitations due to Rabi splitting when compared to the bare system. The effect of the cavity remains relevant even when the time-scale for reaching the final ME state is long compared to typical cavity lifetimes of tens of femtoseconds. The reason for this is that the cavity resonance merely produces the doorway state through which the external light enters the system, and the passage through this state towards the various intermediate states may be shorter than the cavity lifetime.

A closer look at the dynamics starting from the UP and LP states is provided in Fig. 4. Following the excitation of the UP, most of the population rapidly transitions to the LP and the dark exciton (cf. Eq. 7), where it becomes trapped. Following the excitation of the LP, and due to its too low energy in relation to the intermediate states, the population remains

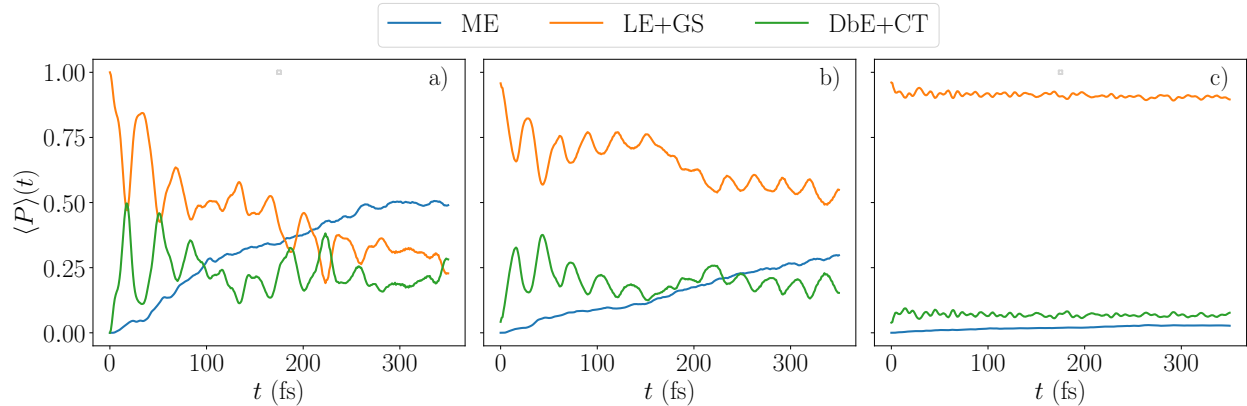


Figure 3: Time evolution of the electronic populations within the dimer. (a) bare and (b, c) cavity-coupled system at coupling strength 0.06. In each case the initial state corresponds to (a) the bright exciton $|0, 1_+\rangle$, (b) the UP $|\psi_+\rangle$ and (c) the LP $|\psi_-\rangle$.

trapped and the SF process is then completely quenched.

Collective Effects

Finally, we consider an ensemble of N molecules (in this case N dimers) and as usual scale down the coupling to the cavity by the factor $N^{-1/2}$ to maintain a constant Rabi splitting, and thus as constant energy of the bright doorway states, in all simulations. The σ TIPS dimer model was extended to include $N = 2$ and 4 molecules. The absorption spectrum for the cases $N = 1, 2, 4$ (cf. Fig. 5a) is virtually identical in the region of the LP resonance, whereas the UP resonance becomes broader as the number of coupled molecules is increased. This broadening is caused by the well-known involvement of the nominally dark polaritonic states, non-adiabatically coupled to the bright states.³⁵ A broadening effect in the UP is equally seen in vibrational strong coupling,⁴⁴ and can be understood as being generated by resonances involving the LP and dark states plus vibrational excitations and the UP. These couplings result in a fast non-radiative relaxation from the UP towards the dark states and the LP.

Correspondingly, the SF yield, i.e. the final ME state population, when starting from the LP is quite insensitive to collective effects. The LP is in all cases off-resonant with the intermediate states and the population remains trapped there, as seen in Fig. 5c. The

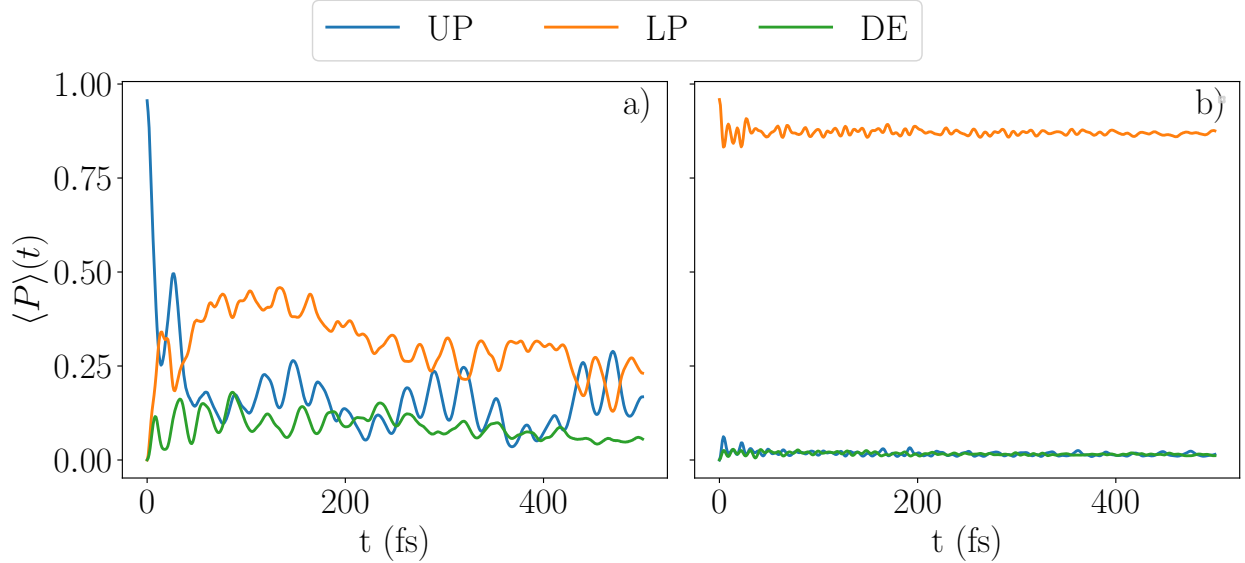


Figure 4: Population of the UP, LP and dark exciton states as a function of time following the excitation to (a) the UP and (b) the LP states of a single dimer coupled to the cavity. The simulations are the same as in Fig. 3.

dynamics starting from the UP are instead sensitive to N because the decay rate towards the dark states and LP depends on the number of molecules.³⁵ In this case, the system relaxes towards the LP and dark states faster for larger N . Interestingly, the fast relaxation towards the dark states manifold, which are energetically equal to the bare dimer excitation, does not result in an increased ME yield. This can be understood from the perspective that the initial excitation energy of the UP quickly redistributes among the vibrational modes as suggested by the broader absorption resonance, thus leading after a few tens of femtoseconds to a similar energetic situation as reached through the direct excitation of the LP.

Upper Polariton as a Doorway State

These results seem to imply that using the UP as a doorway state for SF cannot improve the SF yield. However, the situation in which the LE excitations of the bare system are too low compared to the $^1(T_1T_1)$ state is rather common,¹⁹ and in this case a modified resonance condition that uses the UP to couple to the final ME might enhance the yield.

In order to investigate this possibility thoroughly, we reduced the oTIPSm to only the

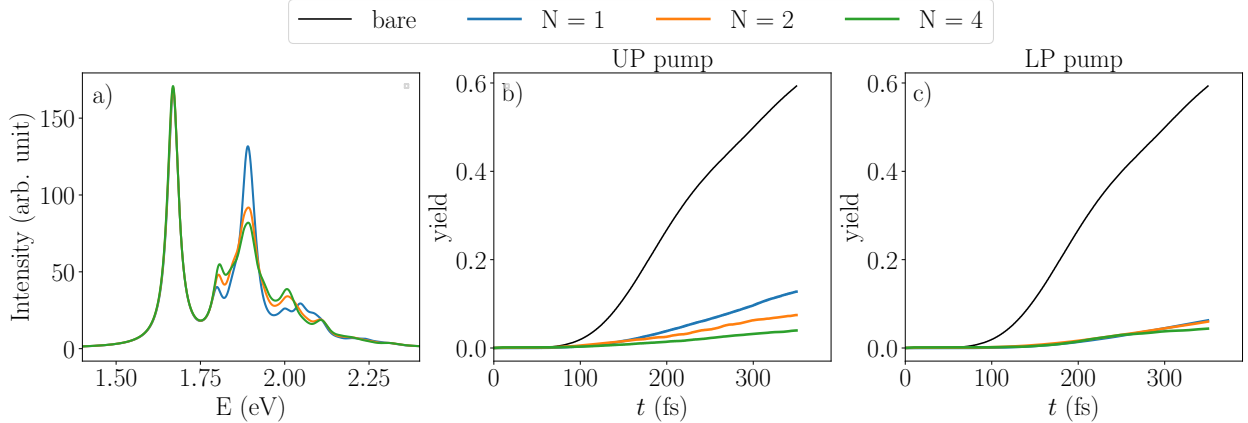


Figure 5: (a) Absorption spectra for a set light-matter coupling strength for one, two and four dimer molecules in the cavity with $g/\omega = 0.04$. Calculated TT yield after pumping the UP (b) or the LP (c) for 1,2 and 4 molecules. The fast Rabi oscillations were smoothed by a running average over 10 data points

main tuning Q_{19} mode but kept all 8 electronic states of each dimer (This model corresponds to the simulations shown in Fig. 5b in Ref. 32). We then shifted the energy of the LE states down by about 0.1 eV until no noticeable population transfer to the ME state occurs in the bare system. This corresponds to an energy gap of 1.73 eV between the electronic ground state and the LE excitation. For this model, the cavity parameters were varied within the frequencies 1.6 – 2.0 eV in 0.01 eV steps and the light-matter coupling strength was varied in the range 0.045 – 0.090 in 0.005 steps, thus resulting in 396 parameter combinations. Each parameter combination underwent relaxation to the ground vibro-polaritonic state, and a corresponding absorption spectrum was calculated to determine the exact position of the UP resonance. The frequency of the laser ω_L used to resonantly couple to the UP state was then set in each case to correspond to the excitation energy of the center of the UP absorption band. The absorption spectrum corresponding to a few selected parameter combinations together with the spectral distribution of the excitation pulse are shown in Fig. 6.

Most of the parameter space results in close to zero yield, as seen in Fig. 7a. Let us first consider the cavity frequency $\omega_c = 1.7$ eV, the closest value in the parameter space to the resonance frequency of the singlet resonance. Only when the coupling strength reaches about $g/\omega_c = 0.075$ does the population of the ME state reaches a significant percentage

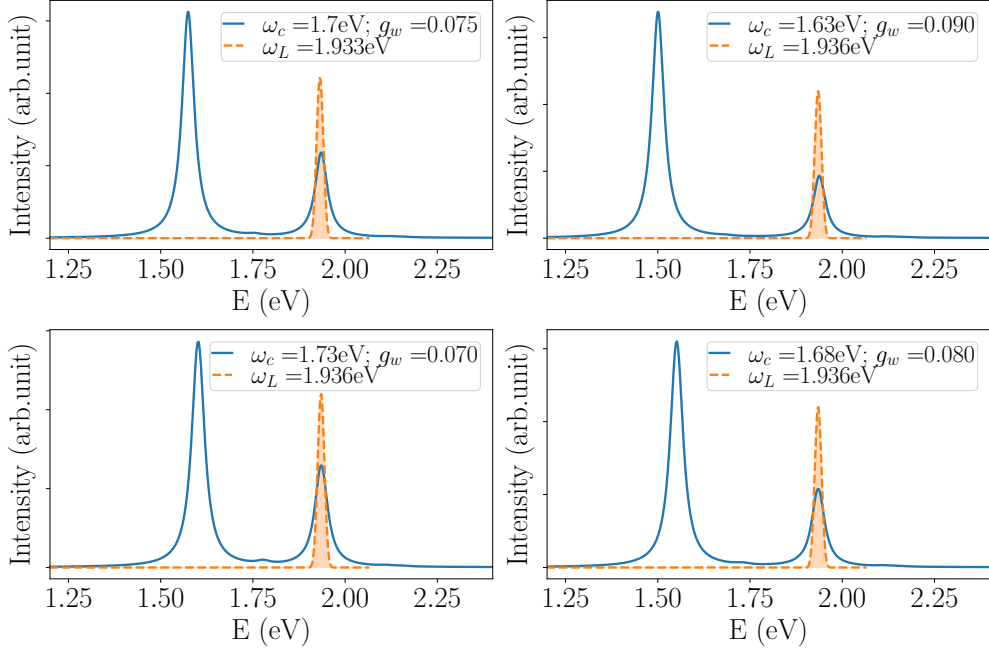


Figure 6: Absorption spectra for some parameter combinations, each with the corresponding laser directed at the UP.

of about 50%. This corresponds to the UP being at the ideal energy to act as a doorway toward the ME final state. If the cavity is tuned toward higher frequency, a correspondingly smaller coupling strength is needed to reach the same optimal UP energy, as illustrated by the nearly linear trend in the yield in Fig. 7a. Since the cavity energy is above the singlet excitation energy, the UP is more photonic than molecular, and the total yield reaches only about 15 to 20%. On the other hand, when the cavity is tuned below the LE resonance in the region of 1.6 to 1.7 eV, an increasingly larger coupling strength is required to bring the UP to its optimal energy for the SF mechanism to operate. However, when this condition is achieved, the UP has now a larger molecular than photonic character, which leads to a larger yield compared to the cavity with a higher frequency. Figures 7b and 7c show the time-dependent population of the UP, LP and ME states for the parameter combinations with the largest yield.

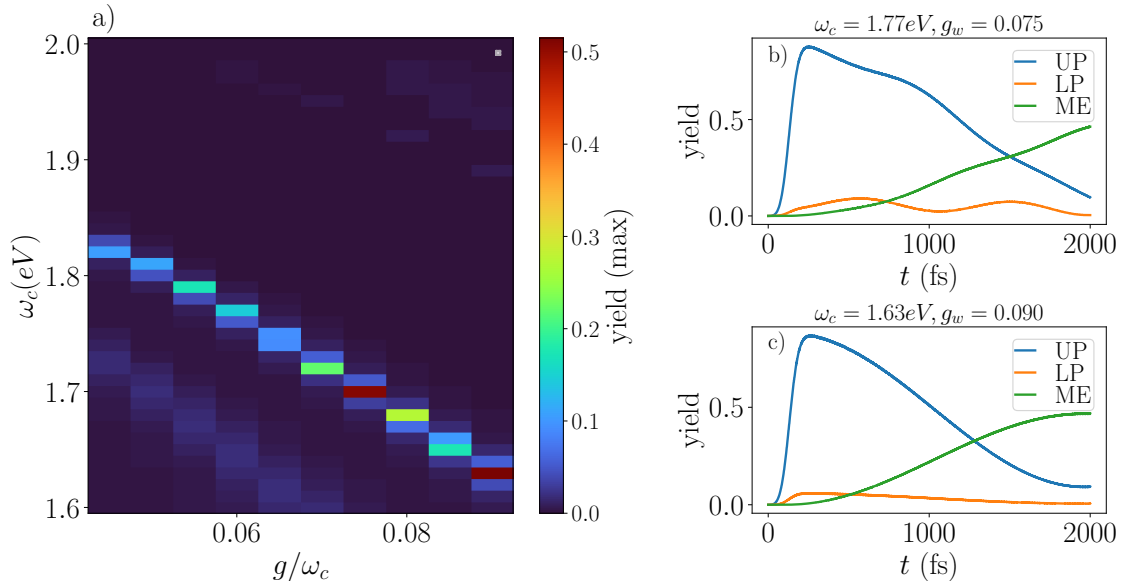


Figure 7: Calculations for the non-optimal singlet fission system for one molecule, (a) shows a systematic scan of different cavity frequencies and coupling strengths and the corresponding ME yield when pumping the UP. (b, c) Time-dependent energy transfer dynamics between the UP, LP and ME states for specific parameters. The fast Rabi oscillations were smoothed by a running average over 10 data points.

Collective Effects in the UP Doorway Mechanism

As mentioned above and as it has been thoroughly analyzed,³⁵ the UP states has an extra open decay channel toward the manifold of $N - 1$ DS and the LP in the presence of N molecules. The influence of this channel on the UP doorway mechanism and possible ways to overcome its negative effect need to be analyzed. When considering this scenario, we weight the coupling strength as usual with $N^{-1/2}$ so that the Rabi splitting is kept constant as a function of N . Figure 8a illustrates the population of the final ME state for the optimal cavity coefficients determined for one molecule and for an increasing number of molecules, where a converged population dynamics has been reached with $N = 8$. The decay channel towards the DS and LP very clearly quenches the SF yield. The efficiency of this relaxation pathway is proportional to the gradient difference between the two electronic states coupled via the cavity, as illustrated in the inset of Fig. 8a. Once the two electronic states become coupled by the cavity, the displaced position of the minima on both PES results in the

resonance condition becoming dependent on the displacement of the vibrational modes, which results in the vibro-polaritonic coupling.

A natural way to counter this decay channel is to demand that the PESs of the electronic ground state and the LE state coupled by the cavity are as parallel as possible. This is a problem of molecular structure and design that has to be solved by considering adequate modifications of the specific molecular scaffolds in chemical space.⁴⁵

Here we consider the modification of the model by shifting the ground electronic state horizontally along the vibrational mode until the gradient difference vanishes. This case is illustrated in Fig. 8b. First of all we see here that the $N = 1$ case has a substantially smaller yield than in the non shifted case. We should note that all electronic states are coupled to each other (cf. Table 1) and that shifting the ground state fundamentally changes the model, such that direct comparisons are no longer possible. Now, however, the decay pathway from the UP towards the DS and LP is not operative and the yield does not decrease with N . Instead, one observes that, in this model, the yield increases with N . One must take this with a grain of salt because as just mentioned, all states including the intermediate CT and DE states are coupled among each other. As the ground state has been moved parallel to the LE states, other side effects may have occurred leading to the observed behaviour. What one can clearly conclude is that a small gradient difference between the cavity coupled states permits the UP state to remain operative as the doorway state, and that realizing this mechanism becomes a question of finding adequate molecular systems.

Conclusions

We considered process of intramolecular singlet fission in *o*-TIPSm dimer, previously studied theoretically by Reddy and Thoss,³² under the effect of strong light-matter coupling in a cavity. This system presents a complex SF mechanism involving the participation of several intermediate CT and DE states mediating the population transfer the final ME

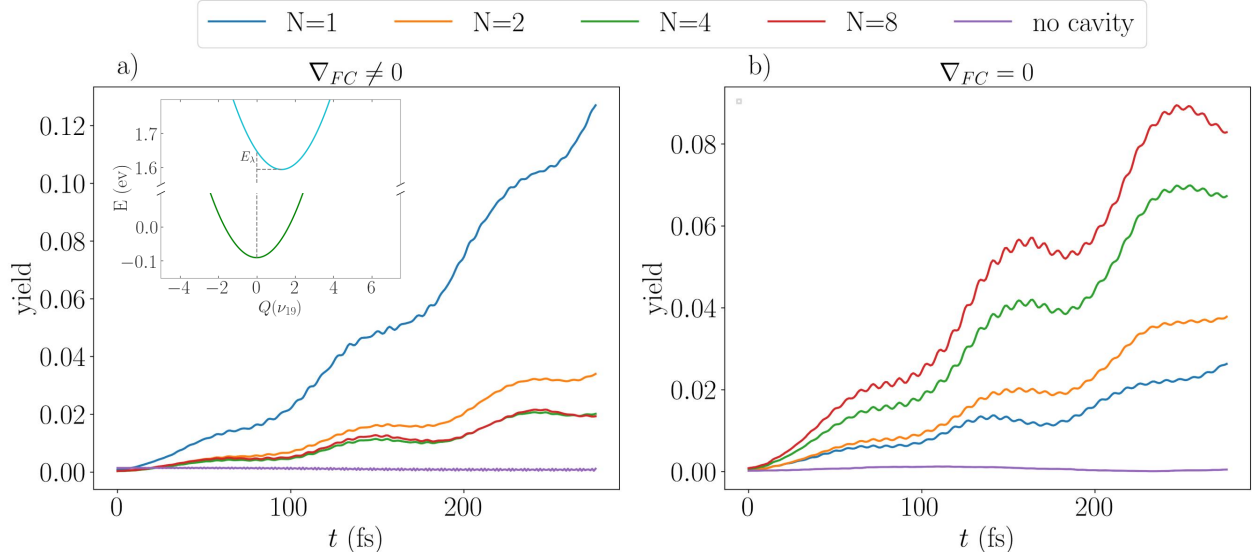


Figure 8: Time evolution of the $^1(T_1T_1)$ yield after an instantaneous photoexcitation of the UP for different numbers of molecules (N) for the two non-optimal iSF model systems with (a) gradient at the FC point and (b) no gradient at the FC point. The diabatic representation of the first excited state along the vibrational mode and the reorganizations energy are shown on the upper right. The fast Rabi oscillations were smoothed by a running average over 25 data points.

state. Simulations in the cavity indicate that the modification of the excitation energy of the doorway state, the LP and UP in the case of strong coupling, result in a large suppression of the ME yield. This is particularly dramatic for the LP, which at moderate coupling strengths is found too low in energy to result in any significant population transfer toward the intermediate states and finally toward the ME state. The results indicate that the energy of the optically bright states, those directly affected by the cavity, relative to the intermediate states, which are insensitive to it, is the relevant quantity that determines the effectivity of the mechanism.

Subsequently we considered the situation where the LE state is too low compared to the $^1(T_1T_1)$ excitation. This is a common situation that invalidates a large set of molecular structures as SF candidates, but which could be remedied by strong coupling and using the

UP as doorway state. An exhaustive cavity parameter analysis indicates that it is possible to find cavity frequency and coupling strength combinations that can largely restore the SF yield in this case. However, using the UP as the doorway state has the caveat that the fast decay towards the dark states and the LP can jeopardize this possibility. We thus consider the situation in which the non-radiative decay channel from the UP is suppressed by reducing the gradient difference along the vibrational modes between the ground electronic state and the LE state. In this case, the SF mechanism can still operate using the upper polaritonic resonance. It then becomes a search problem in chemical space to identify molecular scaffolds fulfilling, at least to some extent, this condition.

Acknowledgement

O.V. acknowledges the collaborative research center "SFB 1249: N-Heteropolyzyklen als Funktionsmaterialien" of the German Research Foundation (DFG) for financial support.

References

- (1) Byrnes, T.; Kim, N. Y.; Yamamoto, Y. Nat. Phys. **2014**, 10, 803–813, Number: 11
Publisher: Nature Publishing Group.
- (2) Coles, D. M.; Somaschi, N.; Michetti, P.; Clark, C.; Lagoudakis, P. G.; Savvidis, P. G.; Lidzey, D. G. Nat. Mater. **2014**, 13, 712–719, Number: 7
Publisher: Nature Publishing Group.
- (3) Mewes, L.; Wang, M.; Ingle, R. A.; Börjesson, K.; Chergui, M. Commun. Phys. **2020**, 3, 1–10, Number: 1
Publisher: Nature Publishing Group.
- (4) Zhong, X.; Chervy, T.; Wang, S.; George, J.; Thomas, A.; Hutchison, J. A.; Devaux, E.; Genet, C.; Ebbesen, T. W. Angew. Chem. **2016**, 128, 6310–6314, eprint: <https://onlinelibrary.wiley.com/doi/pdf/10.1002/ange.201600428>.

- (5) Fidler, A. P.; Chen, L.; McKillop, A. M.; Weichman, M. L. J. Chem. Phys. **2023**.
- (6) Satapathy, S.; Khatoniar, M.; Parappuram, D. K.; Liu, B.; John, G.; Feist, J.; Garcia-Vidal, F. J.; Menon, V. M. Sci. Adv. **2021**, 7, eabj0997, Publisher: American Association for the Advancement of Science.
- (7) Balasubrahmaniyam, M.; Simkhovich, A.; Golombek, A.; Sandik, G.; Ankonina, G.; Schwartz, T. Nat. Mater. **2023**, 22, 338–344.
- (8) Orgiu, E. et al. Nat. Mater. **2015**, 14, 1123–1129, Number: 11 Publisher: Nature Publishing Group.
- (9) Sokolovskii, I.; Tichauer, R. H.; Morozov, D.; Feist, J.; Groenhof, G. Nat. Commun. **2023**, 14, 6613.
- (10) Estes, V.; Caliò, L.; Espinós, H.; Lavarda, G.; Torres, T.; Feist, J.; García-Vidal, F. J.; Bottari, G.; Míguez, H. Sol. RRL **2021**, 5, 2100308.
- (11) Polak, D. et al. Chem. Sci. **2020**, 11, 343–354.
- (12) Shockley, W.; Queisser, H. J. J. Appl. Phys. **2004**, 32, 510–519.
- (13) Smith, M. B.; Michl, J. Chem. Rev. **2010**, 110, 6891–6936.
- (14) Congreve, D. N.; Lee, J.; Thompson, N. J.; Hontz, E.; Yost, S. R.; Reuswig, P. D.; Bahlke, M. E.; Reineke, S.; Van Voorhis, T.; Baldo, M. A. Science **2013**, 340, 334–337.
- (15) Pensack, R. D.; Ostroumov, E. E.; Tilley, A. J.; Mazza, S.; Grieco, C.; Thorley, K. J.; Asbury, J. B.; Seferos, D. S.; Anthony, J. E.; Scholes, G. D. J. Phys. Chem. Lett. **2016**, 7, 2370–2375, Publisher: American Chemical Society.
- (16) Burdett, J. J.; Bardeen, C. J. Acc. Chem. Res. **2013**, 46, 1312–1320, Publisher: American Chemical Society.

- (17) Zirzmeier, J.; Lehnerr, D.; Coto, P. B.; Chernick, E. T.; Casillas, R.; Basel, B. S.; Thoss, M.; Tykwinski, R. R.; Guldi, D. M. PNAS **2015**, 112, 5325–5330.
- (18) Casanova, D. Chem. Rev. **2018**, 118, 7164–7207.
- (19) Padula, D.; Omar, O. H.; Nematiram, T.; Troisi, A. Energy Environ. Sci. **2019**, 12, 2412–2416.
- (20) Smith, M. B.; Michl, J. Annu. Rev. Phys. Chem. **2013**, 64, 361–386.
- (21) Liu, B.; Menon, V. M.; Sfeir, M. Y. ACS Photonics **2020**, 7, 2292–2301, Publisher: American Chemical Society.
- (22) Takahashi, S.; Watanabe, K.; Matsumoto, Y. J. Chem. Phys. **2019**, 151, year.
- (23) Theurer, C. P.; Laible, F.; Tang, J.; Broch, K.; Fleischer, M.; Schreiber, F. Nanoscale **2023**, 15, 11707–11713.
- (24) Berghuis, A. M.; Halpin, A.; Le-Van, Q.; Ramezani, M.; Wang, S.; Murai, S.; Gómez Rivas, J. Adv. Funct. Mater. **2019**, 29, 1901317.
- (25) Kolesnichenko, P. V.; Hertzog, M.; Hainer, F.; Galindo, D. D.; Deschler, F.; Zaumseil, J.; Buckup, T. J. Phys. Chem. C **2024**, 128, 1496–1504.
- (26) Kolesnichenko, P. V.; Hertzog, M.; Hainer, F.; Kefer, O.; Zaumseil, J.; Buckup, T. Hot electrons and dark excitons modulate strong-coupling conditions in metal-organic optical microcavities. <http://arxiv.org/abs/2401.14835>.
- (27) Martínez-Martínez, L. A.; Du, M.; Ribeiro, R. F.; Kéna-Cohen, S.; Yuen-Zhou, J. J. Phys. Chem. Lett. **2018**, 9, 1951–1957.
- (28) Sun, K.; Gelin, M. F.; Zhao, Y. J. Phys. Chem. Lett. **2022**, 13, 4090–4097.
- (29) Gu, B.; Mukamel, S. J. Phys. Chem. Lett. **2021**, 12, 2052–2056.

- (30) Zhang, B.; Zhao, Y.; Liang, W. J. Phys. Chem. C **2021**, 125, 1654–1664.
- (31) Climent, C.; Casanova, D.; Feist, J.; Garcia-Vidal, F. J. Cell Rep. Phys. Sci. **2022**, 3, year.
- (32) Reddy, S. R.; Coto, P. B.; Thoss, M. J. Phys. Chem. Lett. **2018**, 9, 5979–5986.
- (33) Ulusoy, I. S.; Gomez, J. A.; Vendrell, O. J. Phys. Chem. A **2019**, 123, 8832–8844.
- (34) Flick, J.; Ruggenthaler, M.; Appel, H.; Rubio, A. PNAS **2017**, 114, 3026–3034, Publisher: Proceedings of the National Academy of Sciences.
- (35) Vendrell, O. Phys. Rev. Lett. **2018**, 121, 253001.
- (36) Wang, H.; Thoss, M. J. Chem. Phys. **2003**, 119, 1289–1299.
- (37) Manthe, U. J. Chem. Phys. **2008**, 128, 164116.
- (38) Vendrell, O.; Meyer, H.-D. J. Chem. Phys. **2011**.
- (39) Manthe, U.; Meyer, H.-D.; Cederbaum, L. S. The Journal of Chemical Physics **1992**, 97, 3199–3213.
- (40) Beck, M. H.; Jäckle, A.; Worth, G. A.; Meyer, H.-D. Phys. Rep. **2000**, 324, 1–105.
- (41) Worth, G. A.; Beck, M. H.; Jäckle, A.; Vendrell, O.; Meyer, H.-D. The MCTDH Package, Version 8.2, (2000). H.-D. Meyer, Version 8.3 (2002), Version 8.4 (2007). O. Vendrell and H.-D. Meyer Version 8.5 (2013). Versions 8.5 and 8.6 contains the ML-MCTDH algorithm. Current versions: 8.4.24, 8.5.17, and 8.6.3 (Jan 2023). See <http://mctdh.uni-hd.de/>.
- (42) Vendrell, O. Chemical Physics **2018**, 509, 55–65.
- (43) Ulusoy, I. S.; Vendrell, O. The Journal of Chemical Physics **2020**, 153, 044108.

- (44) Gómez, J. A.; Vendrell, O. J. Phys. Chem. A **2023**, 127, 1598–1608, Publisher: American Chemical Society.
- (45) Dreuw, A.; Tegeder, P. Physical Chemistry Chemical Physics **2023**, 25, 17079–17091.

Appendix

Calculation details

Figure 9 shows the ML-tree structures for the *o*-TIPS model for two and four molecules. Each molecule has separate vibrational and electronic degrees of freedom. All vibrations are represented by a harmonic oscillator DVR using the same grids as in Ref.³² The electronic degrees of freedom and the cavity are represented by general discrete bases.

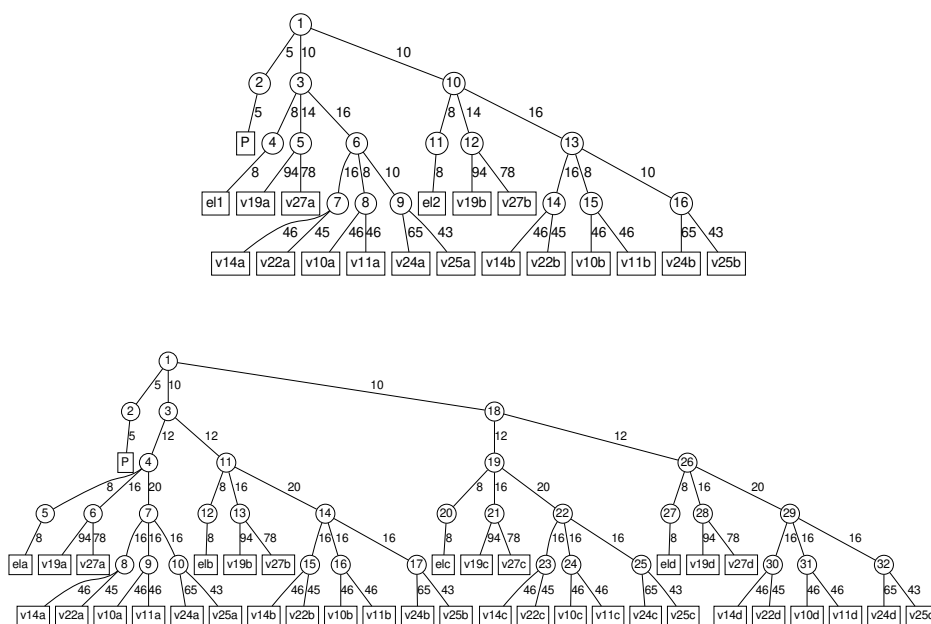


Figure 9: ML-tree structure of the *o*-TIPS model for two (a) and four (b) molecules. The number of each node can be seen in the circles. The number of SPFs per node are given by the number along the branches. The square boxes indicate which degree of freedom it represents and above them the number of primitive basis functions is given.